Since January 2020 Elsevier has created a COVID-19 resource centre with free information in English and Mandarin on the novel coronavirus COVID-19. The COVID-19 resource centre is hosted on Elsevier Connect, the company's public news and information website.

Lung Pathology of Severe Acute Respiratory Syndrome (SARS): A Study of 8 Autopsy Cases From Singapore

TERI J. FRANKS, MD, PEK Y. CHONG, MBBS, FRCPA, PAUL CHUI, MBBS, MRCPATH (FORENSIC), JEFFREY R. GALVIN, MD, RAINA M. LOURENS, BS, ANN H. REID, MA, ELENA SELBS, MD, PHD, COL PETER L. MCEVOY, MC USA, COL DENNIS L. HAYDEN, MC USA, JUNYA FUKUOKA, MD, JEFFERY K. TAUBENBERGER, MD, PHD, AND WILLIAM D. TRAVIS, MD

Severe acute respiratory syndrome (SARS) is an infectious condition caused by the SARS-associated coronavirus (SARS-CoV), a new member in the family *Coronaviridae*. To evaluate the lung pathology in this life-threatening respiratory illness, we studied postmortem lung sections from 8 patients who died from SARS during the spring 2003 Singapore outbreak. The predominant pattern of lung injury in all 8 cases was diffuse alveolar damage. The histology varied according to the duration of illness. Cases of 10 or fewer days' duration demonstrated acute-phase diffuse alveolar damage (DAD), airspace edema, and bronchiolar fibrin. Cases of more than 10 days' duration exhibited organizing-phase DAD, type II pneumocyte hyperplasia, squamous metaplasia, multinucleated giant cells, and acute bronchopneumonia. In acute-phase DAD, pancytokeratin staining was positive in hyaline membranes along alveolar walls and highlighted the absence of pneumocytes. Multinucleated cells were shown to be both type II pneumocytes and macrophages by pancytokeratin, thyroid transcription factor-1, and CD68 staining. SARS-CoV RNA was identified by reverse transcriptase-polymerase chain reaction in 7 of 8 cases in fresh autopsy tissue and in 8 of 8 cases in formalin-fixed, paraffin-embedded lung tissue, including the 1 negative case in fresh tissue. Understanding the pathology of DAD in SARS patients may provide the basis for therapeutic strategies. Further studies of the pathogenesis of SARS may reveal new insight into the mechanisms of DAD. HUM PATHOL 34:743-748. © 2003 Elsevier Inc. All rights reserved.

Key words: **severe acute respiratory syndrome, SARS, SARS-associated corona virus, diffuse alveolar damage.**

Abbreviations: **AFIP, Armed Forces Institute of Pathology; DAD, diffuse alveolar damage; RT-PCR, reverse transcriptase-polymerase chain reaction; SARS, severe acute respiratory syndrome; SARS-CoV, SARS-associated coronavirus; TTF-1, thyroid transcription factor-1.**

Severe acute respiratory syndrome (SARS) emerged from Guangdong Province, China, in mid-November 2002. As outbreaks occurred in Hong Kong, Viet Nam, and Singapore, the SARS-associated coronavirus (SARS-CoV) swept around the globe via routes of international air travel. Human coronaviruses were first described in the 1960s and are known to cause up to 30% of colds. Although the infectious agent of the SARS epidemic is apparently new, injury to the lower respiratory tract secondary to coronavirus infection is not unprecedented. Wheezing in asthmatic children and acute lower respiratory tract disease in infants and military recruits have been associated with coronaviruses in the past.[1-4] To help improve understanding of the lower respiratory tract injury in SARS, we describe the microscopic findings in 8 patients who died from SARS during the Singapore outbreak.

MATERIALS AND METHODS

Autopsy material from 8 SARS patients, accessioned at the Armed Forces Institute of Pathology (AFIP) from Tan Tock Seng Hospital, Singapore, formed the basis of this study. Clinical and autopsy reports were reviewed. Hematoxylin and eosin–stained slides of lung tissue were reviewed on each patient (range, 3 to 108 slides; mean, 27 slides) for multiple histological features (Table 1). These features were scored as present (+) or absent (−) and, when present, were graded for percentage of tissue involved (1, 1% to 24%; 2, 25% to 49%; 3, 50% to 74%; 4, 75% to 100%) and degree of involvement (1, mild; 2, moderate; 3, marked).

In 8 cases, representative tissue sections of lung prepared from paraffin blocks were stained with Brown-Brenn gram stain, Brown-Hopps gram stain, Ziehl-Neelsen for acid-fast bacteria, and Grocott's methenamine silver for fungi. Microorganisms were determined to be present (+) or absent (−).

Immunohistochemical staining (Table 2) was performed on paraffin-embedded tissue of a representative section of lung from each case. The antibodies were pretreated when necessary with protease or heat-induced epitope retrieval. This was followed by automated immunostaining with either the Ventana stainer (Ventana Medical Systems, Tucson, AZ) using the avidin-biotin-peroxidase complex technique or the

From the Department of Pulmonary and Mediastinal Pathology, Department of Radiologic Pathology, Division of Molecular Pathology of the Department of Cellular Pathology and Genetics and Division of Tropical and Infectious Disease Pathology of the Department of Tropical and Infectious Diseases, Armed Forces Institute of Pathology, Washington, DC, USA; Department of Pathology and Laboratory Medicine, Tan Tock Seng Hospital, Singapore; and Center for Forensic Medicine, Health Sciences Authority, Singapore. Accepted for publication June 18, 2003.

Address correspondence and reprint requests to Teri J. Franks, MD, Department of Pulmonary and Mediastinal Pathology, Armed Forces Institute of Pathology, 6825 16th Street NW, Bldg. 54, Room M003B, Washington, DC 20306.

0046-8177/03/3408-0003$00.00/0
doi:10.1016/S0046-8177(03)00367-8

TABLE 1. Histologic Features of the Lung in 8 Autopsy Cases of SARS

Case Number	1	2	3	4	5	6	7	8
Sex/age	F/67	M/63	M/43	M/38	M/68	M/50	F/29	M/39
Illness (days)	4	6	8	10	16	16	18	20
DAD, acute	+	+	+	+	+	+	+	+
%	2	4	3	3	1	1	3	1
grade	2	3	2	1	1	1	3	3
Airspace edema	+	+	+	+	+	−	−	−
%	3	4	3	4	2	−	−	−
grade	2	2	3	2	2	−	−	−
Bronchiolar fibrin	+	−	+	+	−	−	−	−
DAD, organizing	−	+	−	−	−	+	+	+
%	−	1	−	−	−	4	4	4
grade	−	1	−	−	−	3	3	3
Pneumocyte hyperplasia	−	+	−	−	+	+	+	+
%	−	2	−	−	1	4	3	4
grade	−	3	−	−	1	2	3	2
Squamous metaplasia	−	+	−	−	+	+	+	+
Multinucleated cells	−	+	−	−	−	+	+	+
Acute bronchopneumonia	−	+	−	−	+	+	+	+
%	−	2	−	−	3	4	2	4
grade	−	1	−	−	1	3	2	3
Infarct	−	−	−	−	−	+	+	−
%	−	−	−	−	−	1	1	−
Hemorrhage	+	−	−	+	+	+	+	+
%	2	−	−	2	1	3	2	3
Fibrin thrombi	−	+	+	−	−	+	+	+
Cytopathic effect	−	−	−	−	−	−	−	−
Hemophagocytosis	−	−	−	−	−	−	−	−
Special stains	−	+	−	−	−	+	−	−
Viral immunos	−	−	−	−	−	−	−	−

%: 1 = 1 − 24%, 2 = 25 − 49%, 3 = 50 − 74%, 4 =75 − 100% parenchymal involvement.
Grade: 1 = mild, 2 = moderate, 3 = marked.

Dako stainer (Dako, Carpinteria, CA) using a link polymer system. Both automated stainers used 3,3'-diaminobenzidine tetrahydrochloride as the chromogen. Negative controls in which the primary antibody was omitted and positive controls on tissues with known positive immunoreactions for each antibody were used. AE1/AE3/CK1 (pancytokeratin), CD68, and thyroid transcription factor 1 (TTF-1) immunostains were studied for multiple histological features. Adenovirus, cytomegalovirus, Epstein-Barr virus latent membrane protein, and herpes simplex virus 1 and 2 immunostains were noted to be positive (+) or negative (−).

At the AFIP, RNA was extracted from formalin-fixed, paraffin-embedded autopsy tissues in 8 cases, as described previously.[5,6] Reverse transcriptase-polymerase chain reaction (RT-PCR) for SARS-CoV RNA was performed using published primers[7] and using methods as described previously.[6] The Defense Medical Research Institute and Singapore General Hospital, Singapore, performed initial RT-PCR tests on fresh autopsy lung tissue in all 8 cases.

TABLE 2. Antibodies

	Pretreatment	Dilution	Source*
Pancytokeratin	Protease	1:400	Chemicon/Dako
CD68	None	1:20	Dako
TTF-1	HIER	1:80	Biocare Medical
ADV	Protease	1:400	Chemicon
CMV	Protease	1:1600	Chemicon
EBV-LMP	Protease	1:400	Dako
HSV 1&2	None	1:200	Cell Marque

*Biocare Medical, Walnut Creek, CA; Cell Marque, Hot Springs, AR; Chemicon, Temecula, CA; Dako, Carpinteria, CA.

RESULTS

The study group comprised 6 men and 2 women, with a mean age of 50 years (range, 29 to 68 years). Seven patients were Asian, and 1 was Indian. One patient had diabetes mellitus (case 2). Clinically, all patients met the World Health Organization case definition for suspected or probable SARS.[8] Presenting symptoms included fever in 8 patients (100%), cough in 4 (50%), shortness of breath in 3 (38%), myalgia in 3 (38%), and diarrhea in 2 (25%). The time from the onset of symptoms to death ranged from 4 to 20 days (mean, 12 days). The Defense Medical Research Institute and Singapore General Hospital found SARS-CoV RNA in 7 of 8 cases. SARS-CoV was detected in 8 of 8 (100%) cases as tested by RT-PCR on postmortem formalin-fixed, paraffin-embedded lung by the AFIP, Division of Molecular Pathology; 1 of these cases was determined to be negative in the Singapore laboratory.

Histological features are summarized in Table 1. Based on duration of illness, several patterns emerge. Cases of shorter duration (10 or fewer days) demonstrated histological features of acute-phase diffuse alveolar damage (DAD), airspace edema, and bronchiolar fibrin. Cases of longer duration (more than 10 days)

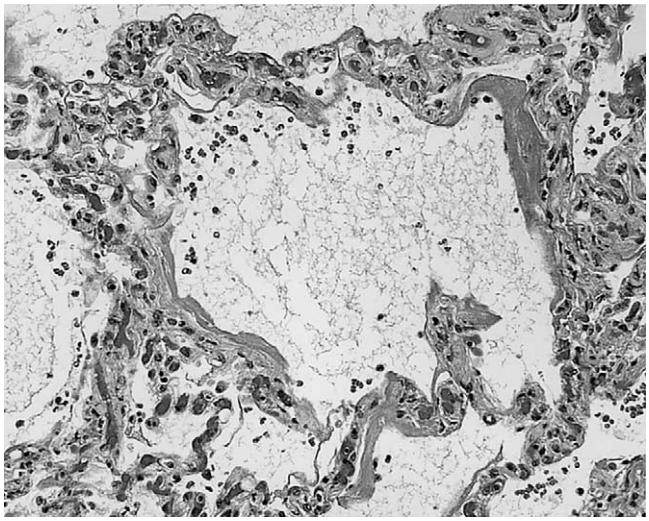

FIGURE 1. Hyaline membranes lining alveolar walls, interstitial and airspace edema, interstitial infiltrates of inflammatory cells, and vascular congestion characterize acute-phase DAD.

demonstrated features of organizing-phase DAD, type II pneumocyte hyperplasia, squamous metaplasia, multinucleated cells, and acute bronchopneumonia. The 1 exception to this pattern was case 2, who was a diabetic.

In cases 1 through 4, cases of shortest duration, acute-phase DAD was present in all 4 (100%), airspace edema in all 4 (100%), and bronchiolar fibrin in 3 of 4 cases (75%). Characterized by hyaline membranes, interstitial and intra-alveolar edema, interstitial infiltrates of inflammatory cells, and vascular congestion (Fig 1), acute-phase DAD involved 50% to 75% of the lung parenchyma and varied in grade from mild to marked. Moderate to marked airspace edema, evidenced by flocculent to solid patches of eosinophilic proteinaceous material within alveolar spaces, involved 50% to 100% of the parenchyma. Bronchiolar injury was demonstrated by collections of fibrin within lumens that were associated with loss of cilia, bronchiole epithelial denudation, and focal deposition of fibrin on exposed basement membranes (Fig 2). Type II pneumocyte hyperplasia was present in only 1 of the 4 patients (25%) in this group. This light microscopy impression was supported by pancytokeratin immunostains, which demonstrated alveolar walls partially covered by hyaline membranes and lacking any type of epithelial lining cells. Hyaline membranes were pancytokeratin positive (Fig 3).

The course of illness was longer than 10 days in cases 5 through 8. Table 1 shows an inverse relationship between the features of early injury described above and those of organization/repair observed later in the course of illness. Organizing-phase DAD, characterized by interstitial and airspace fibroblast proliferation (Fig 4), was accompanied by repair in the form of type II pneumocyte hyperplasia and squamous metaplasia in these 4 patients. Organizing-phase DAD was present in 3 (75%) patients, type II pneumocyte hyperplasia in 4 (100%), and squamous metaplasia in 4 (100%). Organizing-phase DAD involved 75% to 100% of the parenchyma and was graded as marked in the 3 cases affected. In contrast, only 1 patient (case 2) from the group with a shorter clinical course demonstrated organizing-phase DAD. In that instance, the percentage of parenchyma involved was 1% to 25%, and was mild.

Some of the hyperplasic type II pneumocytes showed marked cytological changes, including cytomegaly, nucleomegaly, clearing of nuclear chromatin, and prominent nucleoli. Alveolar spaces contained a combination of macrophages, desquamated pneumocytes, and multinucleated cells. Immunohistochemistry confirmed the presence of CD68-positive macrophages and pancytokeratin-positive/TTF-1–positive type II pneumocytes. Rare multinucleated cells appeared to be either macrophages with CD68 staining or type II pneumocytes with pancytokeratin and TTF-1 staining (Fig 5). No intranuclear or intracytoplasmic viral inclusions were identified. Whereas occasional pneumocytes and macrophages demonstrated fine cytoplasmic vacuoles, vacuolization was not a striking feature in these cases. The numbers of macrophages within alveolar spaces did not appear to be significantly different from the numbers typically seen in non-SARS organizing DAD. Hemophagocytosis was not identified.

Acute bronchopneumonia developed in 4 (100%) patients with clinical courses longer than 10 days. Characterized by accumulations of neutrophils and macrophages within airways and alveoli (Fig 6), the bronchopneumonia involved 50% to 75% of the parenchyma and varied from mild to marked. Sheetlike bacterial growth with areas of hemorrhage and vasculitis, characteristic of *Pseudomonas* pneumonia, was seen on hematoxylin and eosin–stained sections in case 6. Brown-Hopps tissue gram stain demonstrated the presence of thin gram-negative rods, which correlated with postmortem cultures that grew *Pseudomonas aeruginosa.* Post-

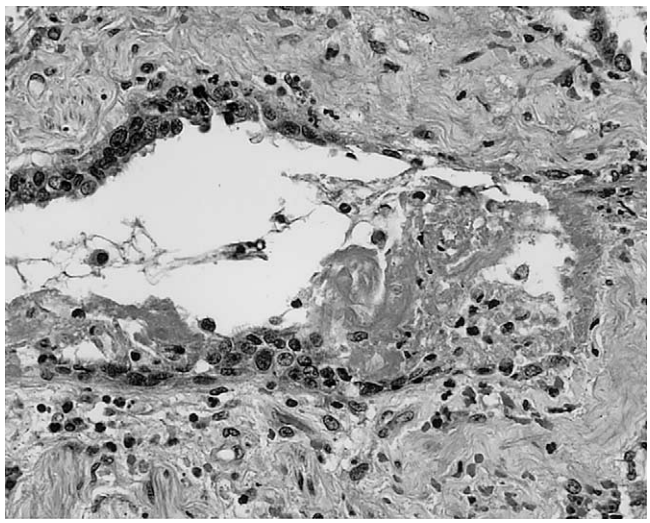

FIGURE 2. Loss of cilia, bronchiole epithelial denudation, and deposition of fibrin within the lumen and on exposed basement membranes signaled injury to small airways.

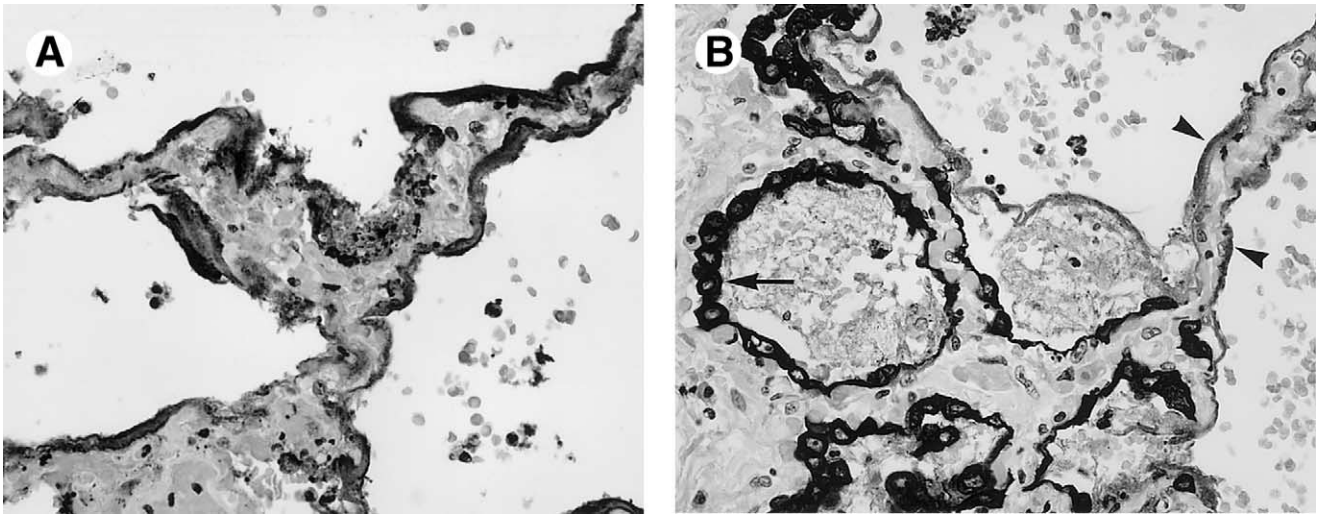

FIGURE 3. (A) Pancytokeratin is strongly positive in hyaline membranes, which cover most, but not all of the edematous alveolar walls. No epithelial lining cells are seen. (B) As repair occurs, hyperplastic type II pneumocytes (arrow) grow over bare alveolar walls (arrowheads).

mortem cultures revealed methicillin-resistant *Staphylococcus aeurus* in case 8. Invasive *Mucor* sp. and *Aspergillus* sp. were identified on Grocott's methanamine silver–stained sections of lung and trachea in case 2. The *Mucor* was observed in a single 2-cm focus of necrotizing bronchopneumonia and exhibited angioinvasion. The *Aspergillus* formed a pseudomembranous and superficially invasive tracheitis (Fig 6). However, these were the only foci of fungal infection in these cases. Immunohistochemistry for the viral agents adenovirus, cytomegalovirus, Epstein-Barr virus latent membrane protein, and herpes simplex virus was negative in all 8 cases.

The remaining histological features included parenchymal infarcts, intra-alveolar hemorrhage, and fibrin thrombi. Although identified in this cohort, these features were present only in a small percentage of cases or were distributed without predilection for either a shorter or longer clinical course. Parenchymal infarcts were present in 2 of 8 (25%) patients, with both cases occurring in the group with clinical courses longer than 10 days. Intra-alveolar hemorrhage was present in 2 of the 4 (50%) patients with shorter illnesses and in 4 of the 4 (100%) patients with longer illnesses. Finally, fibrin thrombi, a common finding in DAD, were seen in the small pulmonary arteries of 2 of the 4 (50%) patients with shorter illnesses and in 3 of the 4 (75%) patients with longer illnesses.

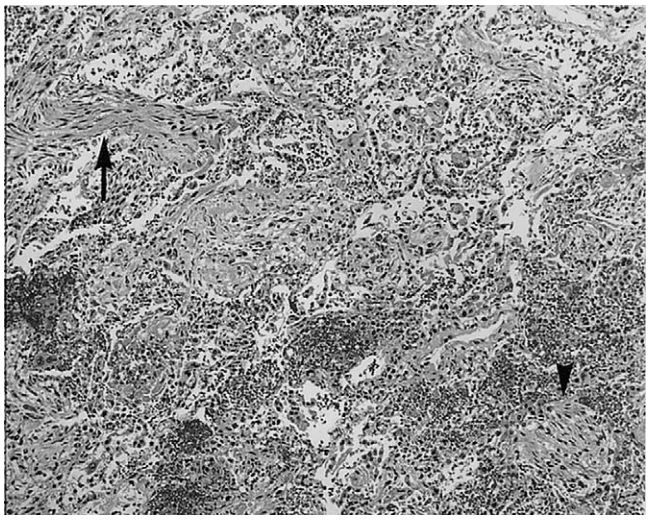

FIGURE 4. In organizing-phase DAD, fibroblast proliferation is seen in the interstitium (arrow) and also in air spaces (arrowheads).

DISCUSSION

In the 8 SARS patients that we studied, the primary pathology in the lung was DAD. The histological correlate of acute respiratory distress syndrome (ARDS), DAD has numerous possible causes, including infections, inhalants, ingestants, drugs, shock, sepsis, radiation, and miscellaneous injuries such as acute pancreatitis, burns, and uremia. Based on our SARS cases, we were able to show a correlation between pulmonary histological findings and the clinical course, with acute patterns of DAD seen in illnesses of 10 or fewer days' duration and organizing patterns of DAD seen in illnesses of more than 10 days' duration. So far, this contrast in histology based on duration of illness has not been emphasized in SARS. This finding generally fits with previously recognized concepts of histological phases of DAD in other settings.[9,10] Given that SARS-CoV has been identified as the cause of SARS,[11] the etiology of DAD in these patients is presumably direct pulmonary epithelial infection by the SARS-CoV. However, the precise mechanism of alveolar wall damage remains to be elucidated.

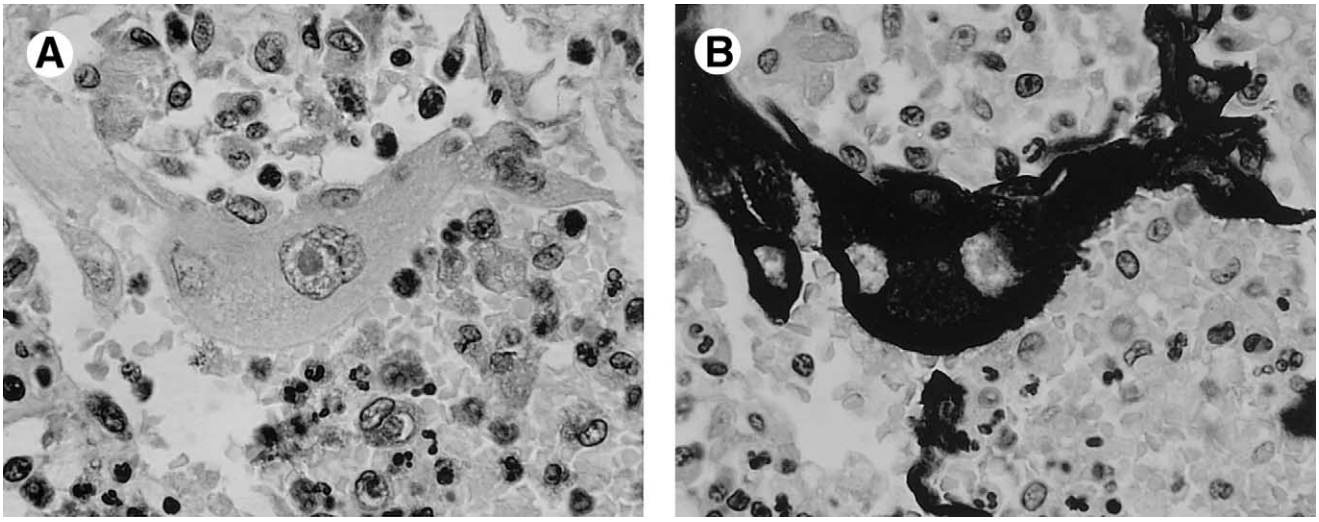

FIGURE 5. (A) Hyperplastic type II pneumocytes display striking cytological atypia including cytomegaly, nucleomegaly, clearing of nuclear chromatin, and prominent nucleoli. (B) Pancytokeratin staining the same multinucleated giant cell is shown. The surrounding cells are a combination of macrophages and neutrophils.

Some viruses can be identified in histological sections by their characteristic tissue response and cytopathic changes. For example, the combination of bronchiolar necrosis and smudge cells is virtually diagnostic of adenovirus pneumonia. Although SARS-CoV did not appear to produce a unique tissue response with characteristic cytopathic changes in this cohort, injury to bronchioles and alveolar epithelium was evident. Three of 4 patients with shorter illnesses demonstrated deposition of fibrin in bronchioles, accompanied by loss of cilia, bronchiole epithelial denudation, and focal deposition of fibrin along the exposed basement membrane, features similar to those described by Nicholls et al.[12] The histological findings of bronchiolar injury correlated with small airway injury characterized by expiratory phase mosaic attenuation on high-resolution chest computed tomography in convalescing SARS patients (Yeun-Chung Chang, MD, and Jeffrey R. Galvin, MD, unpublished data). Interestingly, we saw strong pancytokeratin staining of hyaline membranes in the cases exhibiting acute-phase DAD. No type I or type II pneumocytes were evident on pancytokeratin immunostains beneath the hyaline membranes, suggesting massive type I pneumocyte necrosis. The paucity of pancytokeratin-positive cells lining alveolar walls on immunostaining in these 3 cases suggests that type I pneumocytes had been lost and the reparative function of type II pneumocyte hyperplasia had not yet started. These findings are consistent with recognized patterns of pneumocyte injury and proliferation in DAD,[9,10] as well as the recent description of pancytokeratin staining of hyaline membranes in DAD.[13]

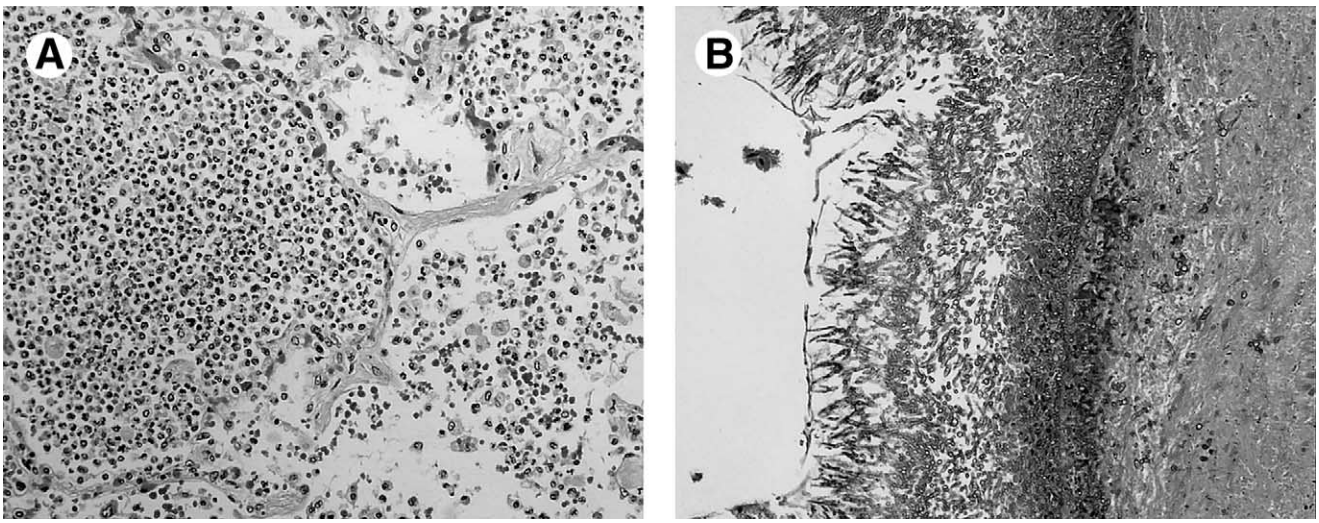

FIGURE 6. (A) Numerous neutrophils and macrophages fill alveoli in acute bronchopneumonia. (B) In addition to acute bronchopneumonia, case 2, a diabetic patient, also demonstrated pseudomembranous and superficially invasive *Aspergillus* tracheitis.

Type II pneumocyte hyperplasia and squamous metaplasia are commonly recognized as reparative features in lung injury, and both can display significant cellular atypia. In the present study, hyperplastic type II pneumocytes showed rather striking cytological changes, including cytomegaly, nucleomegaly, clearing of nuclear chromatin, prominent nucleoli, and multinucleation. Ksiazek et al[14] described cell rounding, a refractive appearance, and cell detachment in Vero E6 cells inoculated with oropharyngeal material from patients with SARS. Examination of the effected Vero E6 cells by electron microscopy revealed characteristic coronavirus particles within the cisternae of the rough endoplasmic reticulum and in vesicles. Although the cytological changes observed in our study may well be viral induced, specific light-microscopy markers of viral infection, such as intranuclear and intracytoplasmic inclusions, were absent. Although severe and suspicious for direct viral effect, the cytological changes seen in our cases were within the spectrum of epithelial changes seen in non-SARS cases of DAD. In the absence of ancillary studies such as immunohistochemistry, the lack of a unique tissue response and cytopathic effect makes the diagnosis of SARS difficult at the light-microscopy level.

The occurrence of multinucleated cells within alveoli in patients with SARS has been previously reported.[12,14,15] Nicholls[12] documented that the multinucleated cells were of macrophage origin in 3 patients and of epithelial origin in 1 patient. We observed multinucleated cells, including CD68-positive macrophages and pancytokeratin-positive epithelial cells, in 4 of our 8 patients (50%). In 1 case the multinucleated cells were also TTF-1 positive, further supporting the epithelial lineage of at least some multinucleated cells. Ksiazek et al[14] have described multinucleated cells, or syncytia, in monolayers of Vero E6 cells infected with the new coronavirus. Although this observation makes a compelling argument for the multinucleated cells representing a cytopathic effect, the histological features of these cells are not unique, and the significance of multinucleated cells in SARS patients is unclear.

Viruses are an important cause of lower respiratory tract disease. Although most viral respiratory infections end in recovery, secondary bacterial infection is a frequent and potentially fatal complication. We observed acute bronchopneumonia in 5 of 8 patients in this study, including 1 patient with a shorter course of illness and 4 patients with longer courses of illness. In the latter group, cultures were positive for *Pseudomonas aeruginosa* in 1 case and for methicillin-resistant *Staphylococcus aureus* in another case. Case 2, with a shorter course of illness, demonstrated invasive *Mucor* in the lung and a pseudomembraneous and superficially invasive *Aspergillus* tracheitis. Coincident diabetes mellitus presumably set the stage for early infection in this patient, and may explain, at least in part, why this is the only case in the short-duration group that showed histological features more typical of cases of longer duration.

In conclusion, the predominant pathology in the lungs of patients infected with SARS-CoV is DAD, a finding present in all 8 patients in this study. DAD is also the pattern of injury seen in convalescing SARS patients (unpublished data). Injury to both bronchiolar and alveolar epithelial cells occurs. Loss of cilia, denudation of the bronchiolar epithelium, and luminal deposition of fibrin provide evidence of injury to the bronchiolar epithelium. Hyaline membrane formation is typically the result of alveolar epithelial necrosis, which is demonstrated in this study by the absence of alveolar lining cells on the pancytokeratin immunostain. Whether the injury to bronchiolar and alveolar epithelium is the primary injury or a secondary phenomenon, and whether the type II pneumocyte multinucleation represents a direct cytopathic effect, remain to be determined.

Acknowledgment. The authors express their gratitude to the staff of the AFIP for their unfailing support in reviewing the extrapulmonary organs in these cases.

REFERENCES

1. McIntosh K, Ellis EF, Hoffman LS, et al: The association of viral and bacterial respiratory infections with exacerbations of wheezing in young asthmatic children. J Pediatr 82:578-590, 1973

2. McIntosh K, Chao RK, Krause HE, et al: Coronavirus infection in acute lower respiratory tract disease of infants. J Infect Dis 130: 502-507, 1974

3. Wenzel RP, Hendley JO, Davies JA, et al: Coronavirus infections in military recruits. Three-year study with coronavirus strains OC43 and 229E. Am Rev Respir Dis 109:621-624, 1974

4. Mertsola J, Ziegler T, Ruuskanen O, et al: Recurrent wheezy bronchitis and viral respiratory infections. Arch Dis Child 66:124-129, 1991

5. Krafft AE, Duncan BW, Bijwaard KE, et al: Optimization of the isolation and amplification of RNA from formalin-fixed, paraffin-embedded tissue: The Armed Forces Institute of Pathology experience and literature review. Mol Diagn 2:217-230, 1997

6. Taubenberger JK, Reid AH, Krafft AE, et al: Initial genetic characterization of the 1918 "Spanish" influenza virus. Science 275: 1793-1796, 1997

7. Drosten C, Gunther S, Preiser W, et al: Identification of a novel coronavirus in patients with severe acute respiratory syndrome. N Engl J Med 348:1967-1976, 2003

8. World Health Organization: Case definitions for surveillance of severe acute respiratory syndrome (SARS). http://www.who.int/csr/sars/casedefinition/en/(accessed June 13, 2003)

9. Katzenstein AL, Bloor CM, Leibow AA: Diffuse alveolar damage—The role of oxygen, shock, and related factors. A review. Am J Pathol 85:209-228, 1976

10. Tomashefski JF Jr: Pulmonary pathology of acute respiratory distress syndrome. Clin Chest Med 21:435-466, 2000

11. World Health Organization: Coronavirus never before seen in humans is the cause of SARS. http://www.who.int/csr/sars/archive/2003_04_16/en/(accessed June 13, 2003)

12. Nicholls JM, Poon LL, Lee KC, et al: Lung pathology of fatal severe acute respiratory syndrome. Lancet 361:1773-1778, 2003

13. Sun AP, Ohtsuki Y, Fujita J, et al: Immunohistochemical characterisation of pulmonary hyaline membrane in various types of interstitial pneumonia. Pathology 35:120-124, 2003

14. Ksiazek TG, Erdman D, Goldsmith CS, et al: A novel coronavirus associated with severe acute respiratory syndrome. N Engl J Med 348:1953-1966, 2003

15. Lee N, Hui D, Wu A, et al: A major outbreak of severe acute respiratory syndrome in Hong Kong. N Engl J Med 348:1986-1994, 2003